Optica Applicata, Vol. LV, No. 3, 2025
DOI: 10.37190/oa/205601

An effective information detection algorithm for low-light images based on the visual perception characteristics of the human eye

Yanchen Liu[1,*], Yefan Shao[2], Hua Li[2], Rong Hou[1]

[1] School of Mechanical and Electrical Engineering, North University of China, Taiyuan 030051, Shanxi, China

[2] School of Life and Environmental Sciences, GuiLin University of Electronic Technology, Guilin 541004, Guangxi, China

[*]Corresponding author: liuyanchenlaoliu@nuc.edu.cn

To solve the problems of low contrast and less effective information of the low-light images, we proposed an effective information detection algorithm based on the visual perception characteristics of the human eye. First, the original image is double-sided filtered to reduce noise and edge preservation. Then, it is converted into the YUV color gamut, and the brightness mapping function is designed to map the brightness channel Y. During the specific mapping process, the overall dark image and the chiaroscuro image are classified according to the brightness variance of the whole image. Different brightness function mappings are designed for each image according to the visual perception characteristics of the human eye so as to realize adaptive brightness enhancement. Experimental results show that the proposed algorithm outperforms the existing algorithms in terms of subjective human eye experience, compared with histogram equalization and the MSR algorithm. It improves the PSNR (peak signal-to-noise ratio), SSIM (structural similarity index metric), and UQI (universal quality index) image quality evaluation indexes by 19.40, 1.17, and 0.77, respectively.

Keywords: visual perception characteristics, brightness function mappings, adaptive brightness enhancement, low-light image enhancement.

1. Introduction

High-quality images carry rich information from captured scenes and can perform advanced computer vision tasks in areas such as autonomous driving, surveillance systems, and advanced driver assistance systems [1-2]. However, when shooting images under poor lighting conditions, such as on a cloudy day or at night, due to insufficient light in the surrounding environment, there is a large number of dark areas in the captured images, and the brightness and contrast ratio are low, resulting in the loss of a large number of details and difficult in obtaining effective information [3].

In nighttime automatic driving of vehicles, the image brightness collected by cameras is often low. Color image processing technology in actual working conditions is generally divided into two categories. One is to extend gray image enhancement technology to color images, such as histogram equalization, adaptive histogram equalization, gamma transform, *etc*. [4-7]. Adaptive histogram equalization significantly enhances the expressiveness of image details through localized contrast enhancement. However, its tile-based processing mechanism is prone to introducing block artifacts, and its sensitivity to noise may lead to over-enhancement in local regions. Additionally, its high computational complexity restricts its applicability in real-time scenarios. Gamma correction, leveraging nonlinear mapping, flexibly modulates the global luminance distribution of images. Nonetheless, the global nature of its single parameter γ renders it incapable of addressing localized illumination variations, often resulting in loss of shadow/highlight details or color distortion. Furthermore, it exhibits limited adaptive capability for complex scenes, failing to dynamically respond to heterogeneous lighting conditions. A key challenge in extending gray image enhancement techniques to color images is maintaining the original colors and preventing distortion [8-9]. The other option is to process color images directly. For example, LAND *et al.* proposed the SSR (single scale retinex) algorithm based on retinex theory [10-11]; however, the single Gaussian scale factor in the SSR algorithm cannot simultaneously take into account image details and image colors. JOBSON *et al.* proposed MSR (multi-scale retinex) algorithm [12]; compared with SSR, the multi-scale Gaussian function retains image details and color information. However, in the actual image enhancement task, the SSR algorithm and MSR algorithm will lead to color image tone offset and overexposure problems.

In view of this, low-light images are taken as the research object, and an effective information detection algorithm is designed for low-light images based on the principle of human visual perception. We first distinguish the overall dark and chiaroscuro images based on the variance of the overall brightness. Additionally, we enhance the two types of images based on the contrast perception characteristics of the human eye in various visual regions. The Hermite interpolation polynomial is used to fit the luminance mapping curve during dark image enhancement at the intersection of light and dark, significantly enhancing the brightness of the dark area.

Meanwhile, the brightness of the bright area remains unchanged so that the brightness of the transition area can enable a natural transition. The proposed algorithm is of great significance and practical value for improving the performance of imaging equipment.

2. Algorithm design

2.1. Algorithm principle

Aiming at the problems of color distortion and detail loss in low-light image enhancement, this paper makes a series of designs to solve the corresponding problems, respectively. First, we filter the original image bilaterally, preserving detailed information while removing noise. Color distortion is mostly due to the fact that in the process of brightness enhancement, three channels in the RGB color domain all have brightness information, which makes it impossible to effectively enhance the brightness information in the RGB color gamut but easy to change the color, resulting in color distortion. For this purpose, we convert the image from the RGB gamut to the YUV gamut, and Y in the YUV gamut is a luminance channel. In this way, brightness enhancement can be carried out without changing color information. The night road often faces a variety of luminance environments; it can be summarized as the overall dark and chiaroscuro image, and the corresponding algorithm should be designed accordingly. The classification judgement module is first built by looking at a lot of statistics about the overall dark image and the chiaroscuro image. Then, the difference between the two is found so that the overall dark image and the chiaroscuro image can be told apart by the size of the image variance. Then, corresponding algorithm enhancements are designed for these two types of dark light images, and linear mapping is performed for overall darkness. For images with overlapping brightness and darkness, the Otsu algorithm is used to segment the bright and dark areas in the image and perform partition enhancement, as shown in Fig. 1.

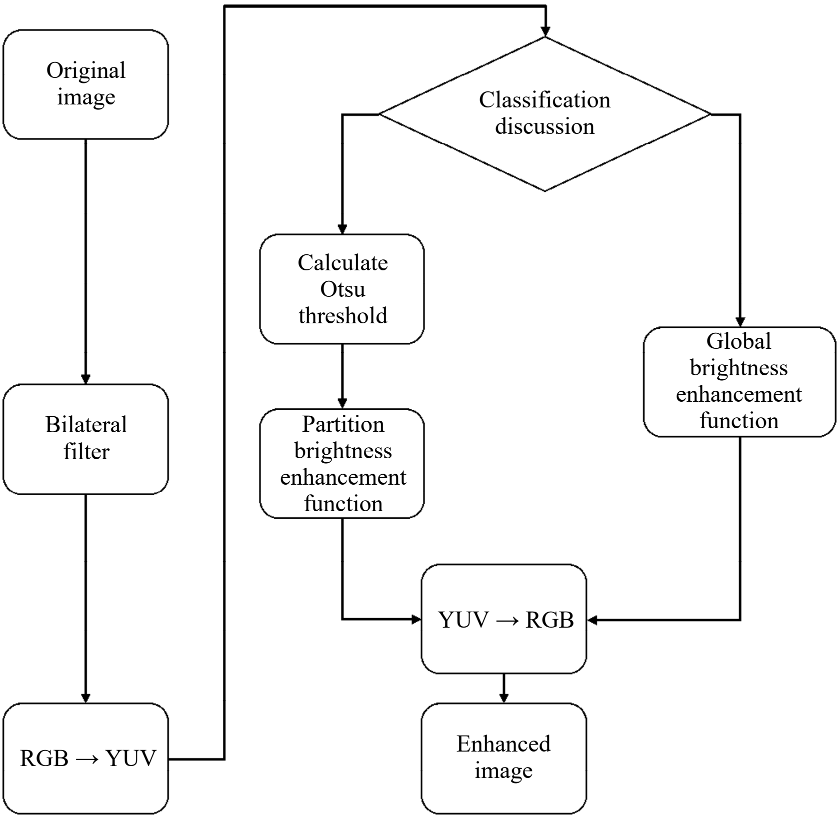

Fig. 1. Algorithm flow chart.

2.2. Overall dark image enhancement

As demonstrated in Formula (1), we can directly perform contrast stretching on the pixel value of the entire dark image. We can multiply the image brightness for linear stretching, which cannot only improve the contrast of the darker image but also increase the brightness.

The human vision system can be described by the human eye's resolution of gray images, which is one of its main characteristics. We can obtain Formula (1) by applying Weber's law to the perception of human brightness.

$$\frac{\Delta B_T}{B} = k \tag{1}$$

where B stands for image background brightness, and ΔB_T stands for JND (just noticeable difference) under this background brightness. According to Formula (1), it can be summarized as follows: When the average brightness of the image increases, the JND also increases. Over a fairly wide range, the k value can be regarded as a constant. It increases significantly when the brightness is very high or very low.

In psychophysics, this phenomenon of JND changing with background is called the luminance masking feature of humans. Human eyes have uneven sensory capacities for varying brightness levels, according to the masking properties of human vision [13-18]. The Buchsbaum curve [19] reflects the relationship between the just noticeable difference ΔB_T of human vision and the background luminance B. To facilitate calculation, we piecewise linearized the Buchsbaum curve according to the ratio of the background luminance to the minimum perceptible luminance. According to the strength of human visual perception, the human eye perception of the region can be divided into dark,

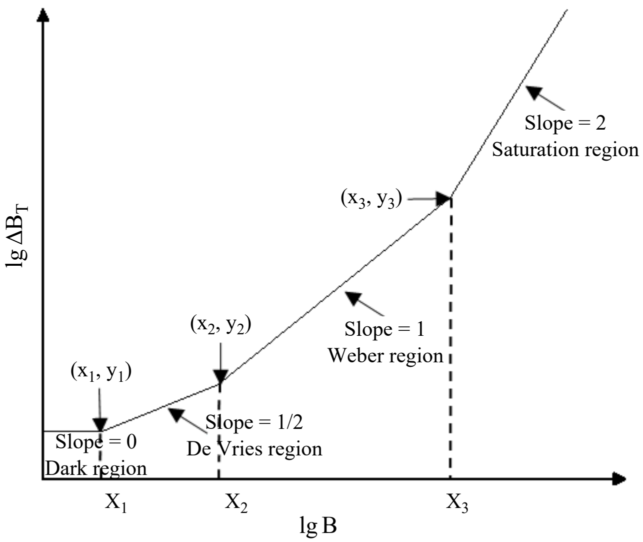

Fig. 2. Simplified Buchsbaum curve.

de Vries region, Weber region, and saturation region. The simplified Buchsbaum curve is shown in Fig. 2.

The region with a slope of about 1/2 is called the De Vries region, which corresponds to the low illuminance region of the image. The region with a slope of 1 in the middle section of the curve is the Weber region, which is a region where the difference can be felt obviously if the stimulus intensity is not high and corresponds to the medium illuminance region of the image. The high illumination region of the image is defined as the saturated region, which is affected by stimulus saturation. The slope of this region is usually greater than 1. The rest is the low-contrast area where the human eye cannot feel the light change.

According to this division, an image can be seen as a combination of dark, De Vries, Weber, and saturated regions. Because the brightness is too dark in the De Vries region, human eyes can recognize but cannot accurately obtain the details of the image. Image information can be reflected normally and intuitively in the Weber region image, and human eyes can easily perceive image details.

The image in the saturated area is too bright so human eyes cannot accurately obtain the image details. The dark area corresponds to the part of the image where the brightness is too low for the human eye to get information at all. The Weber region area is larger in the image, and the image details are clearer and the visual effect is better. According to the overall dark images shown in Fig. 3, the histogram analysis was carried out as shown in Fig. 4.

Most of the pixel values in these images are significantly below 200. We count all pixel sizes and then find a pixel value that is just greater than 98% of the other pixels

Fig. 3. Overall dark image.

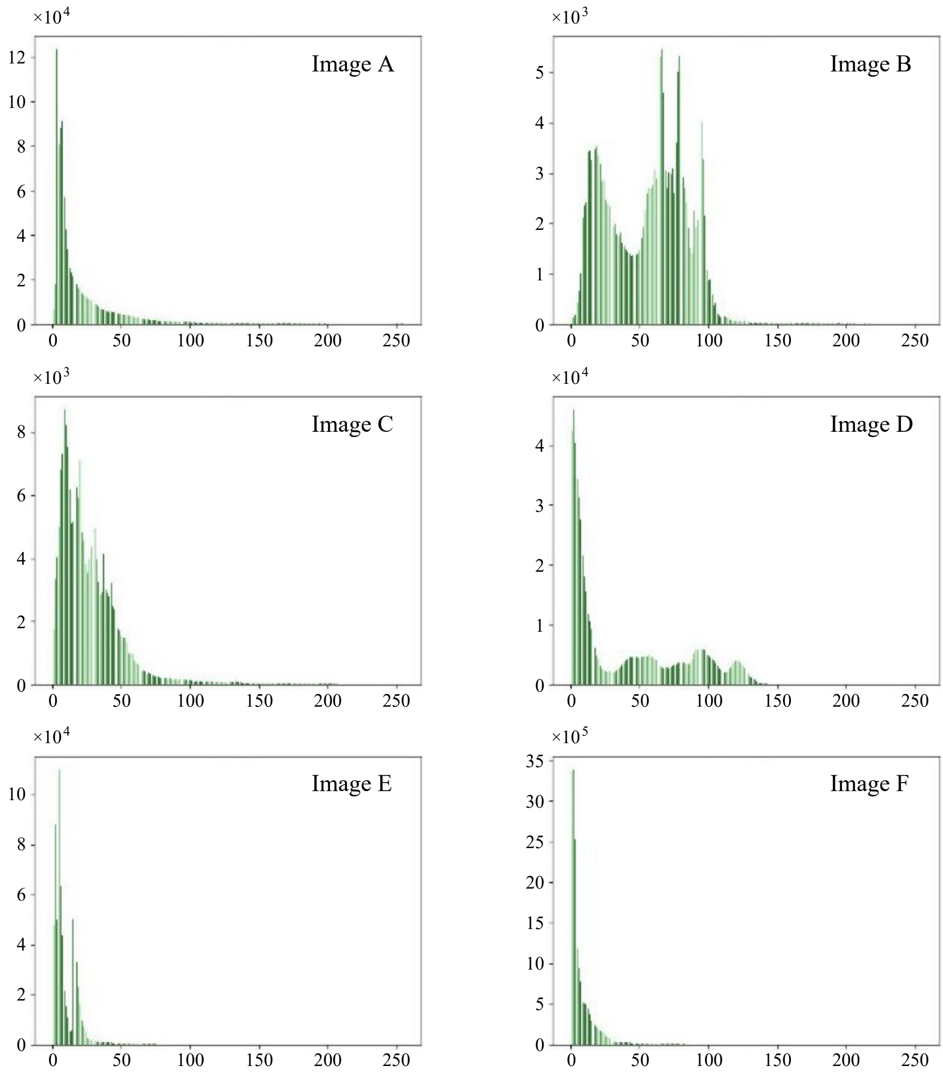

Fig. 4. Histogram of the overall dark image.

in the image, defining it $I_{98\%}$ as the maximum value of the darker area. Based on the statistics in Table 1 and the histogram in Fig. 4, it can be said that the parameter $I_{98\%}$ can fairly and accurately show the maximum value of the darker region.

In Table 1, most of the pixels whose brightness value is lower than $I_{98\%}$, are located in the De Vries region, so we can carry out a linear mapping of the image, and $I_{98\%}$ is

Table 1. The maximum value of the darker area $I_{98\%}$ of different images.

	Image A	Image B	Image C	Image D	Image E	Image F
$I_{98\%}$	110	95	89	97	50	54

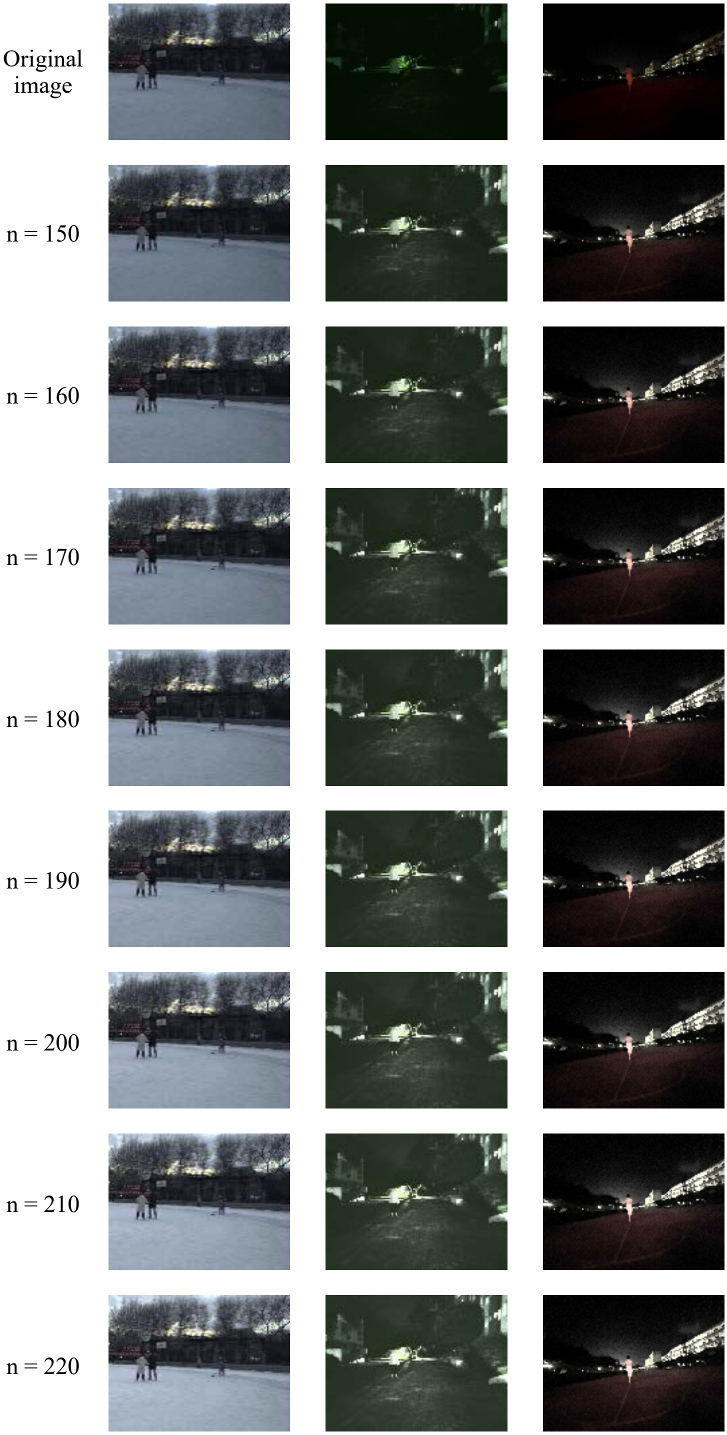

Fig. 5. Critical value test of Weber and saturation region.

mapped to the junction of the Weber region and the saturated region. Only 2% of the images, scattered in the Weber and saturated regions, respectively, are small and negligible. Therefore, we simplify the algorithm and use the following formula to map the entire image linearly:

$$y = kx \tag{2}$$

Among them, k can be determined by:

$$k = \frac{n}{I_{98\%}} \tag{3}$$

where n is the critical value of the interface between Weber region and saturated region, and it is found through experiments that it is most appropriate when $n = 170$, as shown in Fig. 5.

In this way, we can enhance adaptive brightness of the overall dark image. The algorithm increases the contrast of all the pixels in the image based on the linear mapping function of the overall dark image enhancement. This not only makes the image look better, but it also brings out the important details in the image.

2.3. Chiaroscuro image enhancement

For the chiaroscuro image, the light region and dark region in the image are segmented by the Otsu (optimize maximum between-class variance) algorithm [23]. The linear contrast enhancement is taken for dark areas. However, brightness enhancement for dark areas alone will cause large cracks at the junction of light and dark areas. It is necessary to take into account the coordination of light and dark areas in brightness enhancement. Therefore, the segmented conversion function is designed as

$$y = \begin{cases} kx, & 0 < x < \delta \\ H(x), & \delta < x < n \\ x, & x > n \end{cases} \tag{4}$$

In the brightness value from δ to n, it is necessary to reduce the influence of dark region enhancement on this region as soon as possible. Therefore, in this region, a function with a slope of -1 at the coordinate $(\delta, k\delta)$ is designed to make sure that it can return to the curve of $y = x$ as soon as possible, so as to minimize the effect of brightness enhancement on bright areas. At the same time, the slope is 1 at the coordinate (n, n), so that the brightness of pixels near the saturated region remains unchanged.

It is a Hermite interpolation problem. The construction of the Hermite interpolation polynomial approximates the original function, resulting in a single solution for the curve. The Hermite interpolation polynomial is given by:

$$H(x) = k\delta\alpha_0(x) + n\alpha_1(x) + (-1)\beta_0(x) + 1 \cdot \beta_1(x) \tag{5}$$

where

$$\alpha_0 = \left(1 - \frac{x-\delta}{n-\delta}\right)^2 \left(1 + 2\frac{x-\delta}{n-\delta}\right) \tag{6a}$$

$$\alpha_1 = \left(1 - \frac{n-x}{n-\delta}\right)^2 \left(1 + 2\frac{n-x}{n-\delta}\right) \tag{6b}$$

$$\beta_0 = (x-\delta)\left(1 - \frac{x-\delta}{n-\delta}\right)^2 \tag{6c}$$

$$\beta_1 = (x-n)\left(1 - \frac{n-x}{n-\delta}\right)^2 \tag{6d}$$

By substituting Formula (5) into Formula (4), we can obtain a complete chiaro-sculatory image processing function

$$y = \begin{cases} kx, & 0 < x < \delta \\ k\delta\alpha_0(x) + n\alpha_1(x) + (-1)\beta_0(x) + 1 \cdot \beta_1(x), & \delta < x < n \\ x, & x > n \end{cases} \tag{7}$$

According to the analysis of Formula (7), where n is a constant and n is 170 in the previous experiment, δ can be calculated in advance each time, so only k affects the brightness enhancement of the image.

3. Experiment and result analysis

To verify the detection effect of this algorithm on the effective information of low-light images, the experimental environment is PyCharm Community Edition 2022.2.1, and the programming language is Python 3.9, the computer CPU is Intel Core i7-12700H, and the memory is 16GB. The operating system is the Windows 11 Home Chinese V version. The experimental results are shown in Figs. 6 and 7.

Meanwhile, in order to more intuitively feel the superiority of the proposed algorithm over the existing algorithms, the experiment is conducted by comparing it with other common algorithms, such as the histogram equalization algorithm and the MSR algorithm, to get Figs. 8 and 9.

3.1. Subjective evaluations

Figure 6 is the result of the enhancement experiment in the overall dark environment. Figure 7(a) shows a street scene. After the brightness enhancement, the overall brightness improves, allowing you to see more clearly behind the house, pedestrians, and

(a) (b) (c)

Fig. 6. Adaptive brightness enhancement for the overall dark image.

(a) (b) (c)

Fig. 7. Adaptive enhancement effect of chiaroscuro images.

other details of the image. Figure 6(b) shows the dark road at night, the pedestrians are not easy to see in the original image but become clearer and more obvious after enhancement. Figure 6(c) shows a man running on the playground at night, the original light in the environment is dim. After the image is processed with the proposed algorithm in the whole dark environment, the processed image appears brighter and its details are more pronounced to the human eye. Figure 7 shows the dark and light-dark types of images. Figure 7(a) shows the path under the street lamp. The road under the street lamp is clearly visible, while the road away from the street lamp becomes dim. Figures 7(b) and (c) are nighttime street corners with limited street lighting. This paper's algorithm enhancement allows for a clearer view of some vehicles and road edges in the original dark zone.

3.2. Objective evaluation

This type of image with a dark and light-dark mixture is enhanced by this algorithm compared to the existing histogram equalization and MSR in Figs. 8 and 9. The human

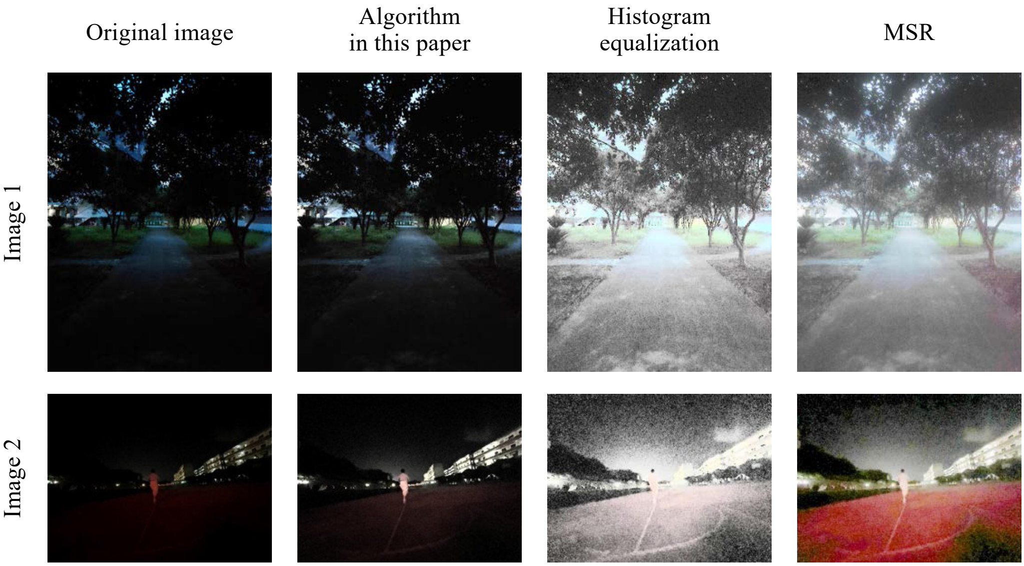

Fig. 8. Image enhancement contrast of the overall dark image.

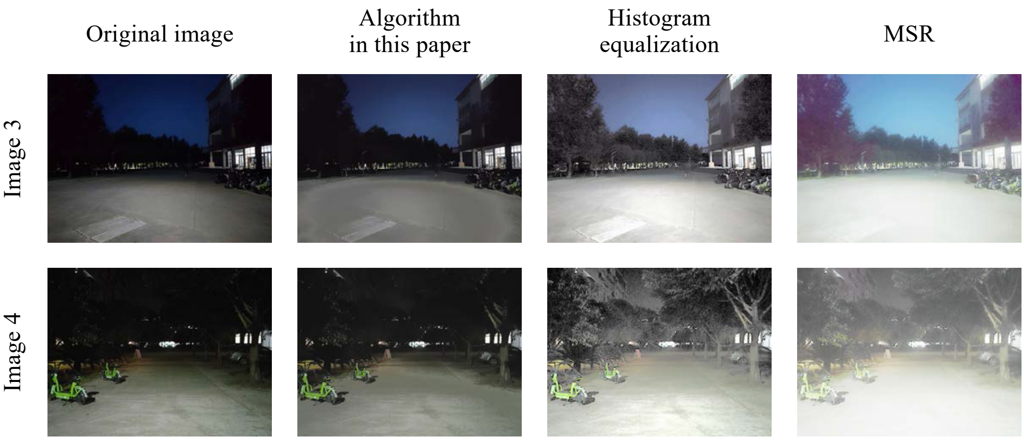

Fig. 9. Image enhancement contrast with chiaroscuro.

eye can intuitively sense that histogram equalization and MSR easily overexpose the image and produce color distortion. The algorithm not only preserves the details but also enhances the brightness, so it offers some advantages.

The subjective evaluation is easily affected by external factors.

1) Peak signal-to-noise ratio (PSNR). It is commonly used to measure the degree of image change. The larger the PSNR is, the smaller the image difference is, the lower the distortion degree is, and the higher the image quality is:

$$\mathrm{PSNR} = 10 \times \lg \frac{\delta^2}{\frac{1}{PQ}\sum_{p-1}^{P}\sum_{q-1}^{Q}\left[f(p,q) - \psi(p,q)\right]^2} \tag{8}$$

where δ represents the rank number of the image, and δ is usually 255; $f(p, q)$ is the initial image; $\psi(p, q)$ is the processed image; p and q are the number of rows and columns in the image, and their sizes remain unchanged after comparison.

2) Universal quality index (UQI). It can be easily calculated and applied to various image processing applications, mainly combined with three factors to calculate, correlation loss, brightness distortion, and contrast distortion. Although the UQI index is defined mathematically and not using the human visual system, a wide variety of image distortions suggest that the UQI is strikingly consistent with subjective quality measures. The UQI index is calculated as follows:

$$\mathrm{UQI} = \frac{4\mu_{\mathrm{O}}\mu_{\mathrm{F}}\sigma_{\mathrm{OF}}}{(\mu_{\mathrm{O}}^2 + \mu_{\mathrm{F}}^2)(\sigma_{\mathrm{O}}^2 + \sigma_{\mathrm{F}}^2)} \tag{9}$$

We also objectively evaluated the images in Figs. 8 and 9, obtaining Tables 2–5. PSNR, SSIM, and UQI are image evaluation indexes. The larger the index value is, the smaller the image distortion is. As shown in the tables, compared with the histogram algorithm, the proposed algorithm improves PSNR by 15.29, SSIM by 0.76,

Table 2. Objective evaluation for test image 1.

	Algorithm in this paper	Histogram equalization	MSR
PSNR	25.12	5.72	6.48
SSIM	1.19	0.03	0.02
UQI	0.86	0.09	0.14

Table 3. Objective evaluation for test image 2.

	Algorithm in this paper	Histogram equalization	MSR
PSNR	19.65	4.91	8.57
SSIM	0.91	0.01	0.03
UQI	0.43	0.02	0.06

Table 4. Objective evaluation for test image 3.

	Algorithm in this paper	Histogram equalization	MSR
PSNR	21.38	9.19	6.29
SSIM	0.87	0.36	0.13
UQI	0.91	0.55	0.45

Table 5. Objective evaluation for test image 4.

	Algorithm in this paper	Histogram equalization	MSR
PSNR	24.90	10.08	6.65
SSIM	0.91	0.45	0.17
UQI	0.97	0.65	0.54

and UQI by 0.47 on average. Compared with the MSR algorithm, PSNR improved 15.52 on average, SSIM improved 0.88 on average, and UQI improved 0.50 on average. The image index corresponding to the proposed algorithm is much higher than that of the histogram and MSR algorithm, which indicates that the image processed by the proposed algorithm has higher contrast, higher brightness, less distortion, more clear image details, and less color distortion, which proves the effectiveness of the proposed algorithm.

4. Conclusions

A new algorithm for effective information detection of low-light images is proposed based on the characteristics of human visual perception.

Firstly, different types of dark light images are judged and classified, and the corresponding algorithms are selected for enhancement, which effectively enhances the adaptability of the algorithm to different types of dark light images. For the overall dark image, the contrast is increased by multiplicative linear stretching, which effectively enhances the brightness of the original image. For images with overlapping light and dark, keep the brightness of the original bright and transition areas roughly unchanged, and enhance the brightness by designing a segmentation function.

Experiments results indicate that the proposed algorithm can preserve the details of the dark areas of the image well, while avoiding overexposure and color distortion. The processing effect is better than the traditional histogram equalization method and the MSR method. It is suitable for effective information detection of low-light images during the driving of ordinary vehicles and is also suitable for other applications that need to enhance low-light images.

Funding

This work was partially supported by the Foundation of Enterprise projects under grant number CD21029X.

References

[1] REN W.Q., LIU S.F., MA L., XU Q.Q., XU X.Y., CAO X.C., DU J.P., YANG M.-H., *Low-light image enhancement via a deep hybrid network*, IEEE Transactions on Image Processing **28**(9), 2019: 4364-4375. https://doi.org/10.1109/TIP.2019.2910412

[2] WANG Y.F., LIU H.M., FU Z.W., *Low-light image enhancement via the absorption light scattering model*, IEEE Transactions on Image Processing **28**(11), 2019: 5679-5690. https://doi.org/10.1109/TIP.2019.2922106

[3] LEE H., SOHN K., MIN D., *Unsupervised low-light image enhancement using bright channel prior*, IEEE Signal Processing Letters **27**, 2020: 251-255. https://doi.org/10.1109/LSP.2020.2965824

[4] KIM Y.-T., *Contrast enhancement using brightness preserving bi-histogram equalization*, IEEE Transactions on Consumer Electronics **43**(1), 1997: 1-8. https://doi.org/10.1109/30.580378

[5] MORONEY N., *Local color correction using non-linear masking*, [In] *IS&T/SID Eighth Color Imaging Conference*, 2000: 108-111. https://doi.org/10.2352/CIC.2000.8.1.art00021

[6] COLTUC D., BOLON P., CHASSERY J.-M., *Exact histogram specification*, IEEE Transactions on Image Processing **15**(5), 2006: 1143-1152. https://doi.org/10.1109/TIP.2005.864170

[7] THOMAS G., FLORES-TAPIA D., PISTORIUS S., *Histogram specification: a fast and flexible method to process digital images*, IEEE Transactions on Instrumentation and Measurement **60**(5), 2011: 1565-1578. https://doi.org/10.1109/TIM.2010.2089110

[8] PIZER S.M., AMBURN E.P., AUSTIN J.D., CROMARTIE R., GESELOWITZ A., GREER T., TER HAAR ROMENY B., ZIMMERMAN J.B., ZUIDERVELD K., *Adaptive histogram equalization and its variations*, Computer Vision, Graphics, and Image Processing **39**(3), 1987: 355-368. https://doi.org/10.1016/S0734-189X(87)80186-X

[9] MURTAZA S.M., AHMAD J., ALI U., *Efficient generalized colored image enhancement*, 2006 IEEE Conference on Cybernetics and Intelligent Systems, Bangkok, Thailand, 2006: 1-5. https://doi.org/10.1109/ICCIS.2006.252334

[10] NAIK S.K., MURTHY C.A., *Hue-preserving color image enhancement without gamut problem*, IEEE Transactions on Image Processing **12**(12), 2003: 1591-1598. https://doi.org/10.1109/TIP.2003.819231

[11] LAND E.H., *The retinex theory of color vision*, Scientific American **237**(6), 1997: 108-129.

[12] LAND E.H., MCCANN J.J., *Lightness and retinex theory*, Journal of the Optical Society of America **61**(1), 1971: 1-11. https://doi.org/10.1364/JOSA.61.000001

[13] BRAINARD D.H., WANDELL B.A., *Analysis of the retinex theory of color vision*, Journal of the Optical Society of America A **3**(10), 1986: 1651-1661. https://doi.org/10.1364/JOSAA.3.001651

[14] JOBSON D.J., RAHMAN Z., WOODELL G.A., *A multiscale retinex for bridging the gap between color images and the human observation of scenes*, IEEE Transactions on Image Processing **6**(7), 1997: 965-976. https://doi.org/10.1109/83.597272

[15] RAHMAN Z., JOBSON D.J., WOODELL G.A., *Multi-scale retinex for color image enhancement*, [In] *Proceedings of 3rd IEEE International Conference on Image Processing*, Vol. 3, Lausanne, Switzerland, 1996: 1003-1006. https://doi.org/10.1109/ICIP.1996.560995

[16] CHIU C.C., TING C.C., *Contrast enhancement algorithm based on gap adjustment for histogram equalization*, Sensors **16**(6), 2016: 936. https://doi.org/10.3390/s16060936

[17] CHEN S.D., *Human visual perception-based image quality analyzer for assessment of contrast enhancement methods*, The International Arab Journal of Information Technology (IAJIT) **13**(2), 2016: 238-245.

[18] PANETTA K., GAO C., AGAIAN S., *Human-visual-system-inspired underwater image quality measures*, IEEE Journal of Oceanic Engineering **41**(3), 2016: 541-551. https://doi.org/10.1109/JOE.2015.2469915

[19] JIA Y., LIN W., KASSIM A.A., *Estimating just-noticeable distortion for video*, IEEE Transactions on Circuits and Systems for Video Technology **16**(7), 2006: 820-829. https://doi.org/10.1109/TCSVT.2006.877397

[20] KUNDU M.K., PAL S.K., *Threshholding for edge detection using human psychovisual phenomena*, Pattern Recognition Letters **4**(6), 1986: 433-441. https://doi.org/10.1016/0167-8655(86)90041-3

[21] PANETTA K.A., WHARTON E.J., AGAIAN S.S., *Human visual system-based image enhancement and logarithmic contrast measure*, IEEE Transactions on Systems, Man, and Cybernetics, Part B (Cybernetics) **38**(1), 2008: 174-188. https://doi.org/10.1109/TSMCB.2007.909440

[22] BUCHSBAUM G., *An analytical derivation of visual nonlinearity*, IEEE Transactions on Biomedical Engineering **BME-27**(5), 1980: 237-242. https://doi.org/10.1109/TBME.1980.326628

[23] XU X., XU S., JIN L., SONG E., *Characteristic analysis of Otsu threshold and its applications*, Pattern Recognition Letters **32**(7), 2011: 956-961. https://doi.org/10.1016/j.patrec.2011.01.021

[24] DE BOOR C., HÖLLIG K., SABIN M., *High accuracy geometric Hermite interpolation*, Computer Aided Geometric Design **4**(4), 1987: 269-278. https://doi.org/10.1016/0167-8396(87)90002-1

[25] TOMASI C., MANDUCHI R., *Bilateral filtering for gray and color images*, Sixth International Conference on Computer Vision (IEEE Cat. No.98CH36271), Bombay, India, 1998: 839-846. https://doi.org/10.1109/ICCV.1998.710815

Received March 28, 2025
in revised form May 12, 2025